An application of normal mode decomposition to measure the acoustical properties of low growing plants in a broad frequency range

Jevgenija Prisutova[a], Kirill Horoshenkov[a], Bruno Brouard[b], Jean-Philippe Groby[b]

[a]*Department of Mechanical Engineering, University of Sheffield, Sheffield, S1 3JD, UK*
[b]*Laboratoire d'Acoustique de l'Université du Maine, UMR6613 CNRS/Univ. du Maine, F-72085 Le Mans Cedex 9, France*

Abstract

This paper presents a new application of the normal mode decomposition to measure the reflection and absorption coefficients of a low growing living plant in a large 300 x 300 mm impedance tube. In this way the higher frequency limit can be extended by a factor of 3 in comparison to that suggested by the standard ISO 10534-2 method for this type of an impedance tube. The adopted method [Prisutova *et al.*, J. Acoust. Soc. Am., 2947-2958, 136, 2014] is based on minimising the difference between the spatial Fourier transform of the measured sound pressure at a range of closely spaced positions along the impedance tube and the predicted transform arising from the normal mode decomposition method. The angular and frequency dependent complex reflection coefficients for the first 5 normal modes are recovered. The acoustical properties of three plants specimen, *Pelargonium hortorum*, *Begonia benariensis* and *Hedera helix*, are measured with the adopted method. These properties are related to the plant morphology through an equivalent fluid model. It is shown that in some cases the predicted and measured data are in close agreement. However, there are cases when the agreement between these data is poor. The possible reasons for this discrepancy are proposed and discussed. This work paves the way for a better understanding of the relations between the plant morphology and its acoustical properties.

PACS: 43.20 Mv, 43.20 Ye, 43.20 El

1. Introduction

Impedance tubes are used widely to determine the ability of materials to absorb sound. The standard procedure for the determination of the absorption coefficient of materials is detailed in the ISO 10534-2 [1]. Porous media are a mostly well understood class of acoustic materials and the relations between the porous microstructure and its acoustical properties are generally well known [2]. However, the acoustical properties of living plants are poorly understood. This information is desirable as there has been strong evidence that some living plants (foliage) are able to absorb a considerable proportion of the energy in the incident sound wave, which makes them attractive for use in noise control elements[3].

The fact that living plants have useful acoustical properties has been known for a while. The original work by Aylor [4] based on field experiments suggested that the ability of crops to attenuate sound waves relates to its leaf area density. Wong *et al*[5] conducted the experiments with different vertical greenery systems, both in field conditions and a reverberation room. They concluded that vertical greenery positively affects the absorption of sound, but more experiments needed to be done on actual building facades for a better understanding of green acoustic insulations. A more recent laboratory work [6] showed that the acoustical properties of low growing plants can be predicted by an equivalent fluid model which is typically used to describe the acoustic behaviour of porous media at low frequencies. In this model the effective flow resistivity was related directly to the leaf area density whereas the tortuosity was related to the dominant angle of leaf orientation[6].

The evidence assembled so far suggests that three main mechanisms are responsible for the absorption of sound by living plants. In the lower frequency range (e.g. below 100-200 Hz) the thermal dissipation mechanisms are important [2]. In the low and medium frequency (e.g. below 1-2 kHz) where the acoustic wavelength is still much larger that the characteristic leaf dimension (e.g. 15-

2

250 mm for typical plants [7]) the viscous dissipation is the prime absorption mechanism [6, 4]. In the higher frequency range (e.g. above 1-2 kHz) where the acoustic wavelength becomes comparable or smaller than the characteristic leaf dimension, the leaf vibration and multiple scattering begin to contribute to the dissipation of the energy in the incident sound wave [7, 4].

There are several reasons by which it is difficult to generalise the results of previous studies to a wider range of low growing plants. A main obstacle to the development of a unified model for sound propagation through foliage is the lack of reliable experimental data on the acoustic reflection/absorption coefficient spectra for a representatively range of acoustic frequencies and angles of incidence. In the field and reverberation chamber experiments which have been reported so far it was difficult if not impossible to deconvolve the acoustic ground effect from the effect of the plant biomass. The reverberation chamber experiments on plants reported so far presented data on the random incident absorption coefficient. Testing large samples of living plants in a laboratory in accordance with the standard ISO 354 method [8] is expensive. It is difficult or impossible to develop from ISO 354 data a general theoretical model for plant absorption which takes into account some morphological characteristics of plants, acoustic frequency and angle of sound wave incidence. Finally, published laboratory work on plants (e.g. by Horoshenkov *et al*[6]) obtained through a controlled experiment in a standard impedance tube presents data for the normal incidence plane wave absorption coefficient determined for a relative small sample area and in a rather limited frequency range.

In this sense, an impedance tube experiment is very attractive. It offers the opportunity to measure the acoustical properties of a plant with great degree of control. However, plants occupy a volume which is greater than that permitted by the cross-section of a standard impedance tube. Therefore, it is of direct interest to be able to measure the acoustical properties of a plant specimen with representative dimensions. This paper attempts to address this issue through the application of an alternative impedance tube method[9] to measure the acoustic absorption of a representatively large specimen of a living plant in

a relatively large impedance tube. In this way, the acoustical reflection and absorption coefficient of this plant can be measured in the frequency range well beyond the first cross-sectional resonance and a range of angles of incidence, as these depend on frequency for higher order modes. An equivalent fluid model is then used together with the independently measured plant morphological data to explain the observed absorption behaviour.

2. Experimental methodology

The reported experiments were carried out using the large impedance tube facilities available at the Laboratoire d'Acoustique de l'Université du Maine (LAUM). A sketch of an experimental setup is presented in Figure 1. It consisted of a square tube which is 4.15 m long and of 300 x 300 mm cross-section at the end of which a plant specimen was installed. The walls of the tube were constructed from 38 mm thick fibreboard panels which were varnished to ensure that they are reflective. One end of the tube was terminated with a 30 mm thick metal lid and at the opposite end three loudspeakers were installed and operated in parallel. The coordinates of their centres were (50 mm, 50 mm), (50 mm, 150 mm) and (150 mm, 150 mm). Such distribution enabled us to excite the maximum number of propagating modes in the adopted frequency range. The signal generated by the three speakers was recorded by a single 1/4" B&K microphone which simulated the axial microphone array in order to avoid amplitude and phase mismatch problems. The movement of the microphone was controlled by a robotic arm. The microphone was placed in the corner of the pipe's cross-section 5 mm away from the wall where the amplitude of all the propagating modes was maximum. The pressure readings were taken at 52 axial positions, distributed with a 40 mm step, with the first reading taken at the interface between a plant and air. As living plants have an uneven surface, the interface was assumed to be at the edge of a leaf farthest from the roots. The data were acquired by a Stanford Research Systems SR785 signal analyser which Fourier transformed the sound pressure signals and stored the pressure

4

spectra in the text file format. According to the ISO 10534-2[1] the maximum frequency of this tube at $T = 20^o$C is $f_u = 0.5c/d = 572$ Hz, where c_i is the sound speed in air and $d = 0.3$ m is the tube dimension. In our work we extended this range to 1800 Hz by using a step-by-step 50-1800 Hz sine sweep and the method detailed in [9]. We recalled this method in Appendix A for the sake of completeness. In accordance with this method the modal reflection coefficients were determined by solving the optimisation problem (eq. (A.4)). The absorption coefficients were then calculated either using the energy ratio (eq. (A.7)) or discrete sound intensity data (eq. A.8)) which were determined with the array of equidistantly spaced microphones. The two methods we used to calculate the absorption coefficient are essentially the same. The only difference is that the former method is continuous, whereas the latter is discrete so that the intensity fit better because of a more accurate determination of the cut-off frequency.
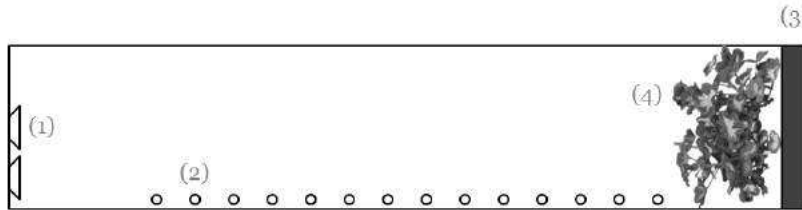
Figure 1: A schematic illustration of the experimental setup: (1) loudspeakers, (2) simulated horizontal microphone array, (3) metal lid, (4) plant specimen.

3. Plant analysis

For the experiments described in this paper, three plant species were used: garden geranium (*Pelargonium hortorum*), begonia (*Begonia benariensis*) and ivy (*Hedera helix*). These plants were purchased from a local garden center in Le Mans (France). Figure 2 shows the photographs of these plants in the pots whereas Figure 3 illustrates the shape and dimensions of their leaves. For the reported experiments plant stems with the foliage were cut off from their

5

roots and placed in the impedance tube with stems parallel (horizontal plant orientation) to the direction of sound propagation. The following morphological characteristics of these plants were measured: mean weight of a single leaf (w_f), mean thickness of a single leaf (h_f), mean area of a single leaf (s_f), number of leaves on a plant (n_f), estimated height of a plant (h_p), and dominant angle of leaf orientation (θ_f). Their values are presented in Table 1. Twenty-five leaves from the geranium plants and twenty leaves from the ficus plants were randomly chosen for the determination of plant characteristics. The weight of leaves was measured using electronic scales the precision of which was ± 0.005 g. The thickness was estimated with the electronic caliper which is capable of measuring distance to ± 0.01 mm. For the leaf area estimation, a picture of a leaf framed by rulers was taken as shown in Figure 3a. Then the picture was imported to Adobe Photoshop software and the amount of pixels in the leaf was determined. Subsequently the leaf area was calculated using the following formula:

$$s_f = p_f \, p_s^{-1} \, s_s \tag{1}$$

where p_f is the number of pixels in a single leaf, p_s is the number of pixels in a reference square and s_s is the area of a reference square. The leaf orientation angles were also estimated using digital images of plants and the screen protractor tool. The above described characteristics were used to derive the following quantities: equivalent volume occupied by the plant (V_p), leaf area per unit volume (A_v), total area of leaves on a plant (s_p), total weight of leaves/stems (w_p), and volume of plant foliage (V_f). These values are presented in Table 1.

4. Equivalent fluid model

In this section we present an equivalent fluid model which we will subsequently use to predict the acoustical characteristic impedance and wavenumber for sound propagation in the foliage. These properties are needed to calculate the angular- and frequency-dependent reflection coefficient and compare it with the measured data for each of the studied plants. The reason why we assume

6

(a) Geranium plant   (b) Begonia plant   (c) Ivy plant

Figure 2: Three types of plant species used in the experiments.
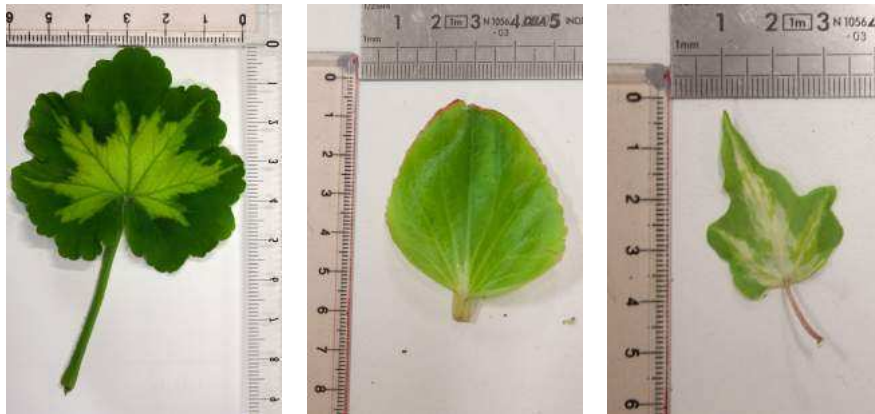
(a) Geranium leaf   (b) Begonia leaf   (c) Ivy leaf

Figure 3: Photographs of leaves of the three plant species used in the experiments.

Plant	w_f (g)	h_f (mm)	s_f (m^2)	n_f (-)	θ_f (degrees)
Geranium	0.794	0.383	0.0020	41	42.6
Begonia	1.010	0.461	0.0032	37	35.9
Ivy	0.124	0.308	0.0006	228	60.9

Table 1: Measured characteristics of plant specimen: average weight of single leaf w_f; average thickness of single leaf h_f; average area of single leaf s_f; number of leaves on plant n_f; dominant angle of leaf orientation θ_f.

Plant	h_p	V_p (m^3)	A_v (m^{-1})	s_p (m^2)	w_p (kg)	V_f (m^3)
Geranium	0.35	0.0079	12.31	0.097	0.0319	0.000055
Begonia	0.18	0.0032	37.76	0.122	0.0390	0.000056
Ivy	0.09	0.0027	51.01	0.138	0.0282	0.000042

Table 2: Calculated characteristics for the three plant specimens in the 300 mm wide square tube: estimated plant layer thickness h_p; equivalent volume occupied by plant V_p; leaf area per unit volume A_v; total area of leaves on plant s_p; total weight of leaves/stems w_p; total volume of plant foliage V_f.

that the reflection coefficient of the plant is angular-dependent is because the effective flow resistivity of the foliage is very low and its porosity is close to 1 (e.g. [6]). In this case it is common to use the extended reaction model in which we consider that the refraction angle at which the sound wave propagates in the foliage depends on the incident angle. The incidence angle in a normal mode depends on the frequency. Therefore it is of importance to model this phenomenon properly. The incidence angle will be shown in those figures which present the modal reflection coefficients we measured in our experiments and calculated with our model.

It was suggested in [6] that the acoustical properties of a low growing plant in a low frequency regime at normal incidence can be represented by an equivalent fluid model, e.g. the empirical model developed by Miki[10]. This model relies on the porosity, ϕ, tortuosity, α_∞, and flow resistivity, σ, which are then

substituted into the following expressions for the characteristic impedance and complex wavenumber in the equivalent volume of fluid occupied by the plant[10]:

$$z_b(f) = \frac{\sqrt{\alpha_\infty}}{\phi} \{1 + 0.070 \left(\frac{f\alpha_\infty}{\sigma\phi} \right)^{-0.632} + 0.107i \left(\frac{f\alpha_\infty}{\sigma\phi} \right)^{-0.632} \}, \qquad (2)$$

$$k_b(f) = \frac{2\pi f \sqrt{\alpha_\infty}}{c} \{1 + 0.109 \left(\frac{f\alpha_\infty}{\sigma\phi} \right)^{-0.618} + 0.160i \left(\frac{f\alpha_\infty}{\sigma\phi} \right)^{-0.618} \}. \qquad (3)$$

where f is the frequency of sound. The characteristic impedance and complex wavenumber are then used to calculate reflection and absorption coefficients of living plants.

The non-acoustical parameters in expressions (3) and (2) were estimated in the following manner. The porosity was estimated from the total volume of the plant foliage, V_f, and volume occupied by the plant, V_p, i.e.:

$$\phi = 1 - \frac{V_f}{V_p}, \qquad (4)$$

The flow resistivity of the equivalent fluid occupied by the plant was estimated using the empirical relations suggested in ref. [6]:

$$\log_{10} \sigma = 0.0083\, A_v + 1.413, \quad \text{for } \theta > 70°, \qquad (5)$$

$$\log_{10} \sigma = 0.0067\, A_v + 0.746, \quad \text{for } \theta < 40°. \qquad (6)$$

where A_v is the leaf area density of the plant and θ is the dominant angle of leaf orientation. The tortuosity was estimated from the knowledge of the dominant angle of leaf orientation[6]:

$$\alpha_\infty = \cos\frac{\theta}{2} + 2\sin\frac{\theta}{2}. \qquad (7)$$

The estimated values of these parameters for the three type of plants adopted for this work are listed in Table 3.

In order to calculate the absorption and reflection coefficients (modal and total) it is necessary to know the values of the characteristic impedance, z_b, and

9

Plant	ϕ [-]	α_∞ [-]	σ [N s/m^4]
Geranium	0.99	1.51	6.74
Begonia	0.98	1.57	9.98
Ivy	0.98	1.57	68.61

Table 3: Estimated non-acoustical parameters for the three plant specimen in the 300 mm tube: porosity, ϕ; tortuosity, α_∞; flow resistivity, σ.

wavenumber, k_b for sound propagation in the foliage. For this purpose we make use of the Miki model (eqs. (2) and (3)). In this case, the normalised acoustic surface impedance and the modal reflection coefficient can then be expressed as:

$$z_s^{mn} = \frac{z_b}{\cos \theta_t^{mn}} \coth(-i\,k_b\,\cos \theta_t^{mn}\,d), \tag{8}$$

$$R_{mn} = \frac{z_s^{mn}\,\cos \theta_i^{mn} - 1}{z_s^{mn}\,\cos \theta_i^{mn} + 1}, \tag{9}$$

respectively. Here θ_i^{mn} is the modal angle of incidence, θ_t^{mn} is the modal angle of refraction and d is the equivalent height of a plant.

The absorption coefficient for the plane wave regime, α_{00}, was then calculated in the following standard manner:

$$\alpha_{00} = 1 - |R_{00}|^2. \tag{10}$$

This acoustical quantity does not account for the energy dissipated by the higher order modes. The ~~modal~~ absorption coefficient defines the amount of energy which is absorbed by one particular mode only and is defined as follows:

$$\alpha_{mn} = 1 - |R_{mn}|^2, \tag{11}$$

where R_{mn} is the modal reflection coefficient, given by expression (9).

The angles at which the higher modes impinged on the porous material surface were calculated separately for each mode by making use of the following

10

formula:

$$\theta_{mn}(\omega) = \arccos\left(\frac{\sqrt{\left(\frac{\omega}{c_0}\right)^2 - \left(\frac{m\pi}{a}\right)^2 - \left(\frac{n\pi}{a}\right)^2}}{\omega/c_0}\right), \qquad (12)$$

where m, n are the indices of the modes propagating in the tube.

5. Results and discussion

This section presents the modal reflection and total absorption coefficients measured with the proposed method. Figures 4 and 5 show the frequency-wavenumber plots for the geranium plant, with the microphone placed in the corner and in the middle of the tube cross-section, respectively. The separation of the first few higher order modes is evident from these plots, which makes them suitable for the subsequent recovery of reflection and absorption information. The frequency-wavenumber plots for the remaining plant specimens show a very similar trend.

Figures 6 and 7 present the predicted (solid line) and measured (black dots) absolute values of the modal reflection coefficients for the geranium specimen, obtained in the corner and in the middle of the cross-section, respectively. The measured data were recovered from the frequency-wavenumber data using the optimisation technique described in Section 3. The predictions for the modal reflection coefficient were calculated according to the method explained in Section 4. The reflection coefficients are plotted as a function of frequency (bottom axis of each subplot) and incidence angle (top axis for higher order modes subplots), which are interrelated as shown in Eq. (12). Figure 6 presents the reflection coefficients for the first four modes, (00), (01), (11) and (02), whereas Figure 7 shows the reflection coefficients of the axi-symmetric modes, (00), (02) and (22). One of the reasons to perform the measurements at two cross-sectional locations was to extend the frequency range where the fundamental mode reflection coefficient can be recovered. Only symmetric modes can be recorded in the middle of the cross-section, and the cut-off frequency of the first axisymmetric mode, (02), is 1143 Hz. This provides a possibility to increase the frequency range

11
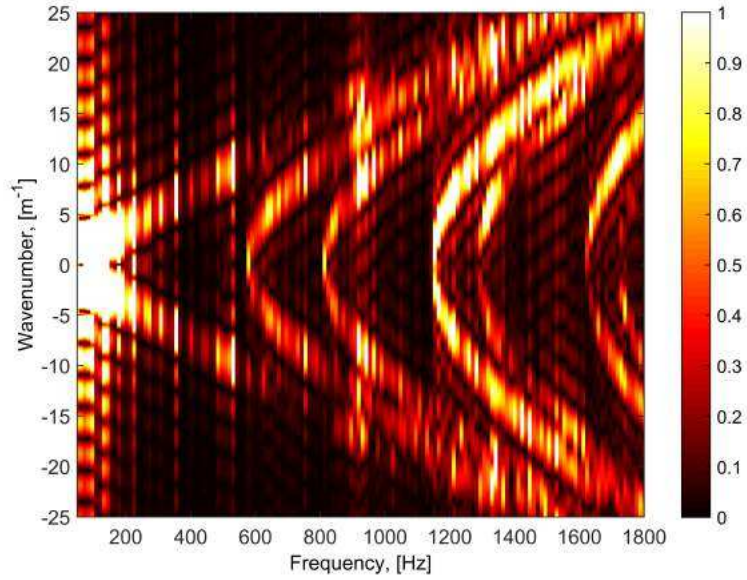
Figure 4: The frequency-wavenumber spectrum for geranium plants measured in 300 mm wide square tube, with the microphone placed in the corner of the tube cross-section.
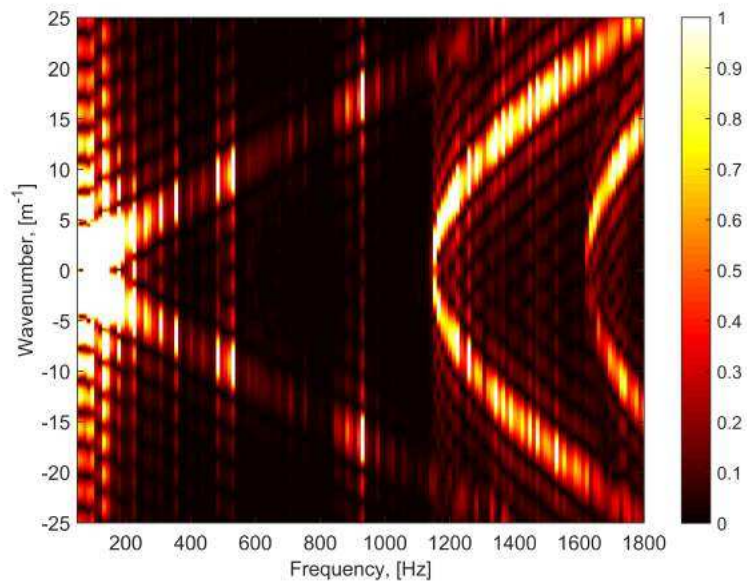
Figure 5: The frequency-wavenumber spectrum for geranium plants measured in 300 mm wide square tube, with the microphone placed in the middle of the tube cross-section.

12

by a factor of two, compared to the cut-off frequency of 572 Hz for mode (01). Although the scattering is still rather strong beyond 572 Hz, the quality of the recovered fundamental mode reflection coefficient in the higher frequency range is better than that recovered with the microphone in the corner of the cross-section. Another important observation is the fact that the model overpredicts the reflection coefficient of mode (00) above the first cross-sectional resonance. This is likely to be attributed to the scattering processes in the greenery, which the model does not account for. For the remaining plants, the reflection coefficient for mode (00) measured in the middle of the tube will be combined with reflection coefficients for modes (01), (11) and (02) measured in the corner of the tube and presented in one figure for each plant.

The mean differences between the measurements and predictions were quantified in accordance with the following equation:

$$\epsilon_{\text{Re}} = \frac{1}{N_q} \sum_{q=1}^{N_q} |\text{Re}(R_{mn}^{(\text{m})}(\omega_q) - R_{mn}(\omega_q))|, \ \epsilon_{\text{Im}} = \frac{1}{N_q} \sum_{q=1}^{N_q} |\text{Im}(R_{mn}^{(\text{m})}(\omega_q) - R_{mn}(\omega_q))|, \tag{13}$$

Here, the error is not normalised as the reflection coefficient only takes values between -1 and 1. The results are presented in Table 4. Generally, the differences are low and they do not exceed the maximum of 10%. This allows for an important conclusion that the proposed plant characterisation method generally works well and it is possible to use it to measure the acoustic behaviour of plants. However, the match for higher modes is worse than that for the fundamental mode, and the model mainly overpredicts the absolute reflection coefficient of the plant above the first cross-sectional resonance frequency (572 Hz). This is likely to signify that the acoustical behaviour of plants above the first cut-off frequency is more complex than that predicted by the model. There is a decrease in the measured reflection coefficient for the angles of incidence in the range of $30° < \theta_{01} < 45°$ for mode (01), which is observed for the three plants. This can happen due to the increase in the effective value of plant tortuosity, calculated via expression (7). Particularly noticeable is the fact that the range of angle corresponds to the dominant angle of leaf orientation of Geranium and Begonia

13
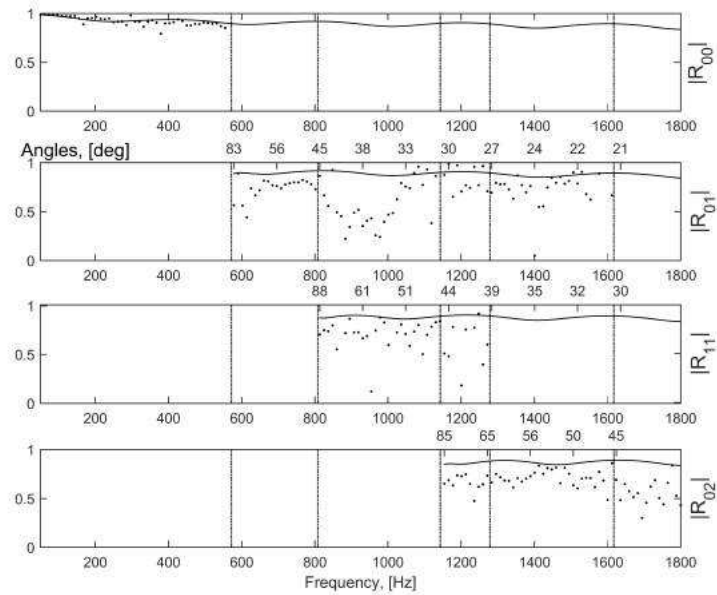
Figure 6: The measured and predicted modal reflection coefficients for geranium plants measured in 300 mm wide square tube, with the microphone placed in the corner of the tube cross-section. Solid line: predictions; dots: experiments.
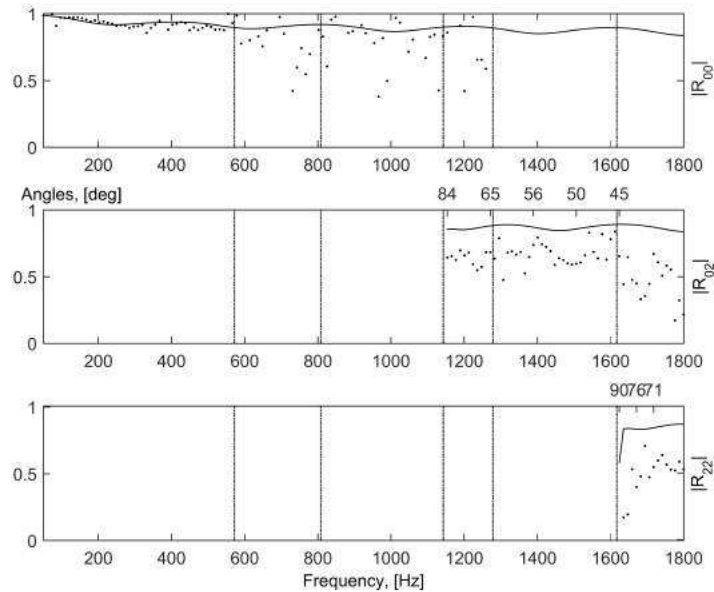
Figure 7: The measured and predicted modal reflection coefficients for geranium plants measured in 300 mm wide square tube, with the microphone placed in the middle of the tube cross-section. Solid line: predictions; dots: experiments.

14
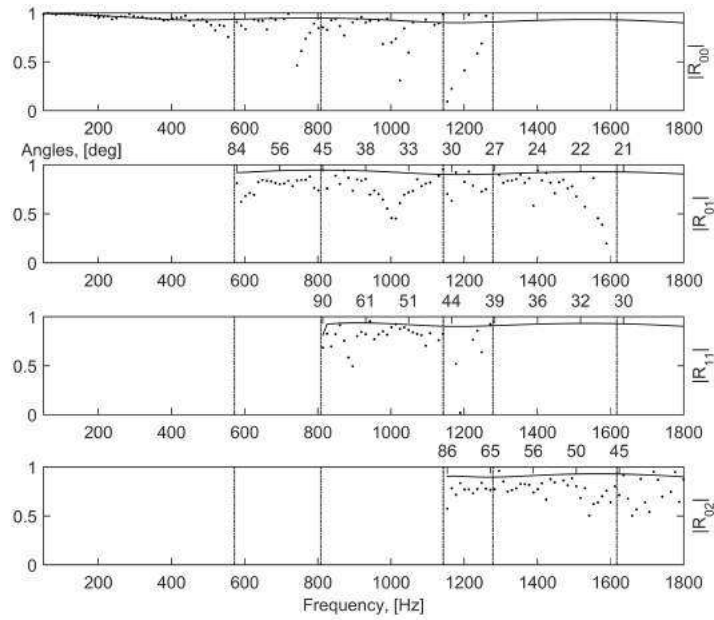
Figure 8: The measured and predicted modal reflection coefficients for begonia plants measured in 300 mm wide square tube, with the microphone placed in the corner of the tube cross-section. Solid line: predictions; dots: experiments.
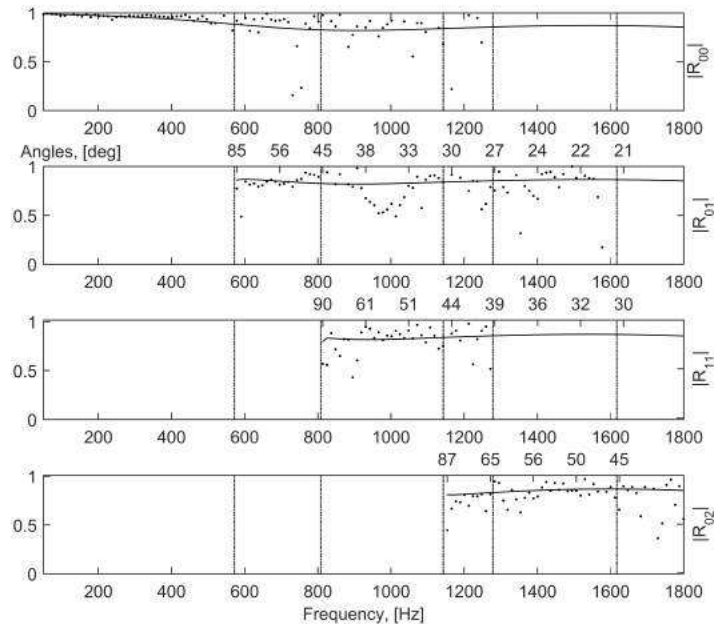
Figure 9: The measured and predicted modal reflection coefficients for ivy plants measured in 300 mm wide square tube, with the microphone placed in the corner of the tube cross-section. Solid line: predictions; dots: experiments.

15

(θ_f is larger for Ivy). It suggests a strong dependence of the density with respect to the orientation of the incident wave. Plant should also be modelled with as

195 an anisotropic material with the equivalent fluid density in the volume occupied by the plant ρ being a 3 by 3 matrix, explaining the discrepancies between the model and the measurement for higher order mode (e.g. see Chapter 10 in [2]).

Plant	$\epsilon_{|R_{00}|}$	$\epsilon_{|R_{01}|}$	$\epsilon_{|R_{11}|}$	$\epsilon_{|R_{02}|}$
Geranium	0.009	0.088	0.043	0.078
Begonia	0.003	0.057	0.016	0.051
Ivy	0.050	0.005	0.001	0.018

Table 4: The mean difference between the absolute values of the measured and predicted modal reflection coefficients for the first four modes for the 300 mm tube.

Figures 10-13 show the measured and predicted values of the total absorp-

200 tion coefficient for the geranium plant in the 300 mm square tube, calculated using Equations (A.7) and (A.8). Figures 10 and 11 present the total absorption coefficients measured in the corner and in the middle of the tube, respectively, and calculated using the incident and reflected amplitudes ratio method, as specified by Equation (A.7). Figures 12 and 13 present the same type of data,

205 but obtained using the intensity method, given by Equation (A.8). The mean differences between the measurements and predictions for these four data sets are shown in Table 5. It is worth noting, that for the incident and reflected amplitude ratio method, the data for each mode were not available throughout the whole frequency range. For example, as it can be seen on the frequency-

210 wavenumber plot for geranium, obtained in the corner of the tube (Figure 4), the dispersion curve for mode (00) disappears after the first cut-off frequency of 572 Hz. This means that the information on the fundamental mode incident and reflected amplitudes was available only in the frequency range between 50 and 572 Hz, instead of 50 to 1800 Hz. Similarly, other modes were also considered

215 in the frequency ranges, where they had a sufficient signal-to-noise ratio. Due

16

to this limitation, two ways of calculating the total absorption coefficient predictions were employed: full theoretical reflection coefficient (full R_{theo}), where each mode exists starting from its cut-off frequency and until the maximum adopted frequency of 1800 Hz, and partial theoretical reflection coefficient (partial R_{theo}), where a frequency range for each mode was matched to that of the measured data. Both of these sets of the theoretical predictions are given in Table 5. However, the partial theoretical reflection coefficient does not reflect the real picture of the sound field in the tube, whereas the full theoretical reflection coefficient cannot be directly compared to the measured data as the latter does not have all the information contained in the theoretical predictions. Due to this issue, it was chosen to use the intensity ratio method for the remaining plants. In addition, Figures 10-13 show the data obtained both in the corner and in the middle of the tube. As the difference between the two is small, for the remaining plants the average total absorption coefficient will be presented.

	$\epsilon_{\alpha_{total}}$
Amp method, corner (full R_{theo})	0.217
Amp method, corner (partial R_{theo})	0.082
Amp method, middle (full R_{theo})	0.144
Amp method, middle (partial R_{theo})	0.007
Int method, corner	0.294
Int method, middle	0.314

Table 5: A summary of the mean differences between the measured and predicted total absorption coefficient for the geranium plant in the 300 mm square tube. Amp method: incident and reflected amplitudes ratio method; Int method: intensity ratio method.

Figures 14 and 15 show the measured and predicted total absorption coefficients for the remaining two plant specimens. It can be seen that for all tested plants the match between the measurements and predictions is close up to the first cut-off frequency. However, the graphs suggest that the model generally underpredicts the absorption by plants beyond this frequency and indicate a

17
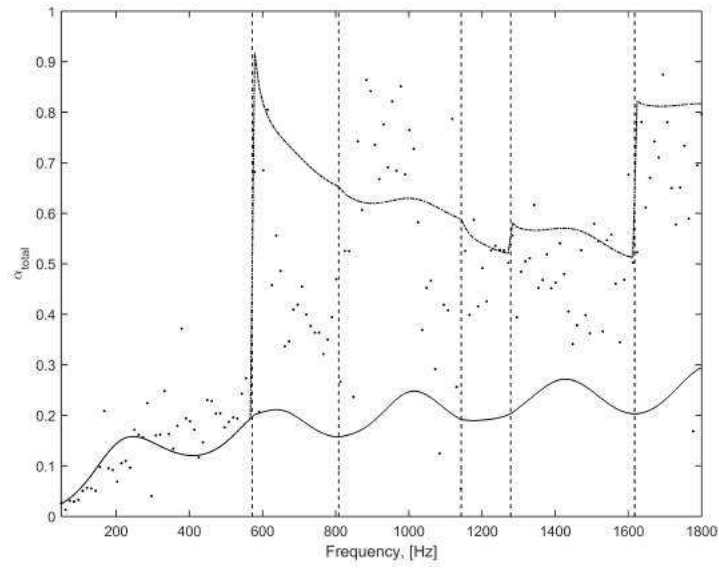
Figure 10: The measured and predicted total absorption coefficients for geranium plants calculated using the amplitude method, measured in 300 mm wide square tube, with the microphone placed in the corner of the tube cross-section. Solid line: full absorption coefficient predictions; dashed line: partial absorption coefficient predictions; dots: experiments.
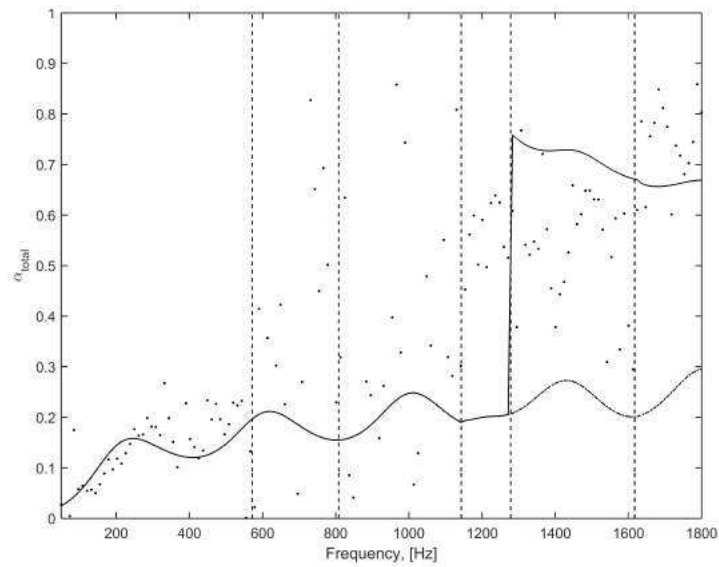
Figure 11: The measured and predicted total absorption coefficients for geranium plants calculated using the amplitude method, measured in 300 mm wide square tube, with the microphone placed in the middle of the tube cross-section. Solid line: full absorption coefficient predictions; dashed line: partial absorption coefficient predictions; dots: experiments.
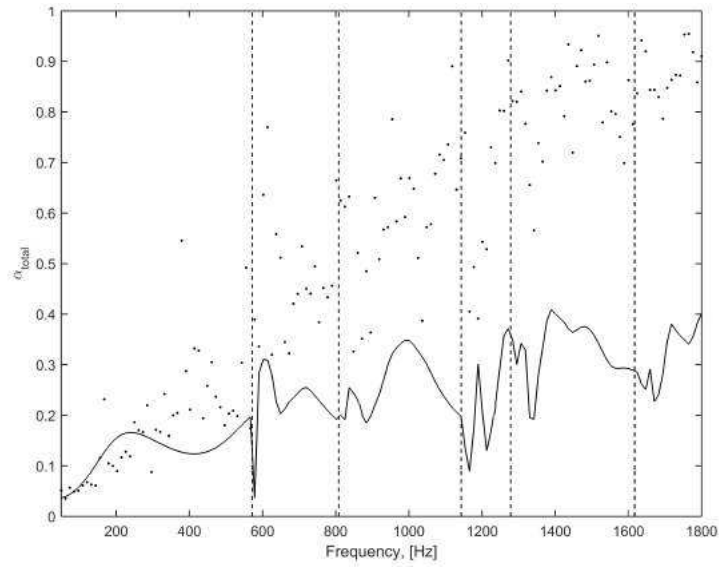
Figure 12: The measured and predicted total absorption coefficients for geranium plants calculated using the intensity method, measured in 300 mm wide square tube, with the microphone placed in the corner of the tube cross-section. Solid line: predictions; dots: experiments.
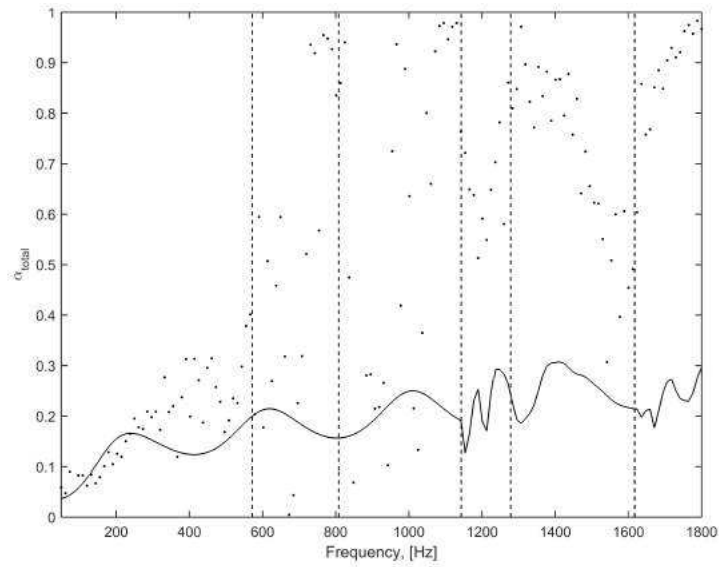
Figure 13: The measured and predicted total absorption coefficients for geranium plants calculated using the intensity method, measured in 300 mm wide square tube, with the microphone placed in the middle of the tube cross-section. Solid line: predictions; dots: experiments.

19

²³⁵ presence of a strong scattering in the tube. As in the case of the reflection coefficients, this discrepancy is caused by the fact that the theoretical model does not take into account the scattering and leaf vibration phenomena, which become stronger as the frequency increases. Also, it can be due to the method - the plants are likely to cause too much scattering which results in the evanescent ²⁴⁰ modes and energy exchange between modes, introducing an error to the phase. Another source of discrepancy at low frequency, is the evidence of anisotropy of plants. The mean leaf orientation was a first step to account for this effect. Obviously the stem direction is one principal direction of anisotropy, associated with the density which is recovered at normal incidence. The determination of the ²⁴⁵ other principal directions is difficult and depends on the mean leaf orientation, assembly of plants and requires additional experiments and further modelling. This affects the quality of the dispersion curves which are subsequently used in the optimisation analysis.

Plant	$\epsilon_{\alpha_{total}}$
Begonia	0.240
Ivy	0.081

Table 6: A summary of the mean differences between the measured and predicted total absorption coefficient for the two plant specimens in the 300 mm square tube.

6. Conclusions

²⁵⁰ The application of a new method[9] to measure the reflection and absorption coefficients of a larger specimen of a living plant in an impedance tube which lateral dimensions are larger than the acoustic wavelength was studied in this paper. The new method is based on measuring the sound pressure spectra with a horizontal microphone array and then applying the spatial Fourier transform ²⁵⁵ to these data to separate the waves incident on plants specimen and the waves reflected from them. It has been shown that in this way the high frequency limit
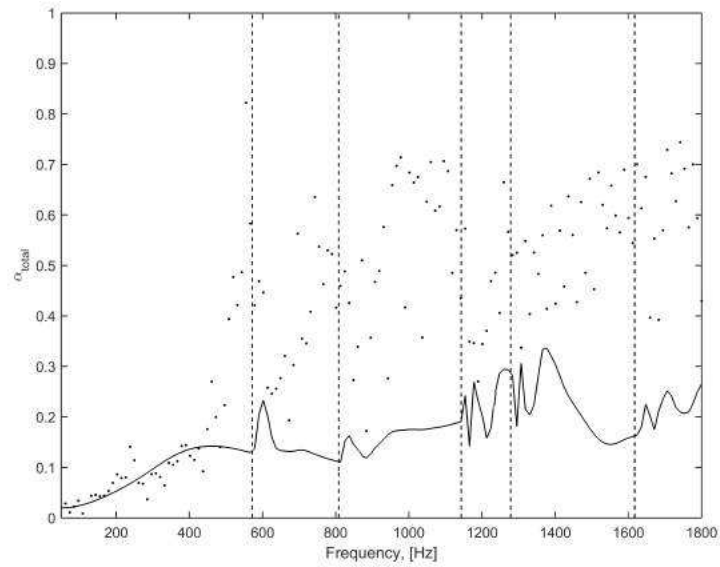
Figure 14: The measured and predicted total absorption coefficients for begonia plants measured in 300 mm wide square tube. Solid line: predictions; dots: experiments.
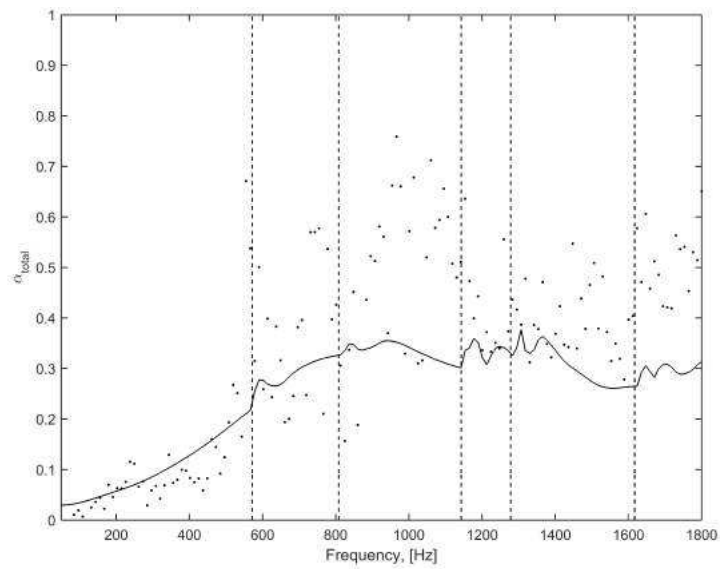
Figure 15: The measured and predicted total absorption coefficients for ivy plants measured in 300 mm wide square tube. Solid line: predictions; dots: experiments.

21

of a rectangular impedance tube can be extended at least by a factor of 3. This allows to measure the acoustical properties of much larger material specimens well beyond the high frequency limit that is currently set in the commonly used ISO 10534-2 standard[1]. The new method also enables us to determine in the laboratory the acoustical properties of a living plant at a range of angles of incidence.

The geranium, begonia and ivy plants have been used to test the proposed method and obtain the complex reflection coefficients and the absorption coefficients. The acoustical properties of plants were characterised using the Miki model [10]. The mean differences between the measured and predicted modal reflection coefficients were less than 10%, and less than 25% for the total absorption coefficients. The agreement between the measured and predicted data becomes worse beyond the first cut-off frequency and a few improvements to the new method can be proposed. Firstly, the residual absorption of the impedance tube needs reducing. This can be achieved by using denser, harder and more reflecting walls of the tube. It is particularly difficult to account for this type of absorption in the case of the higher order modes. Secondly, the experimental procedure can be improved by taking measurements over a longer distance along the tube, in smaller steps and higher spacial accuracy. Thirdly, the theoretical model needs improving to account for more complex absorption behaviour of a living plant in the higher frequency range. In this respect, the adopted equivalent fluid model does not take into account the leaf scattering, vibration phenomena which become more pronounced in living plants as the frequency increases, and anisotropy. These phenomena cannot be neglected in order to achieve a better match between the measured and predicted data. In particular the development of a anisotropic model, allowing to account for the principal direction of propagation is a future step, which first requires the determination of the elements of the density matrix.

Appendix A. Theoretical background

In what follows we briefly recall the measurement and analyse procedure presented in [9]. The sound pressure as a function of frequency ω in a square waveguide with an absorbing termination such as a living plant specimen can be expressed as a superposition of an infinite number of normal modes[11]:

$$p(z, \omega) = \sum_{m=0}^{\infty} \sum_{n=0}^{\infty} \cos \frac{m\pi}{a} x \cos \frac{n\pi}{a} y \left(A_{mn} e^{-ik_{mn}z} + A_{mn} R_{mn} e^{ik_{mn}z} \right), \quad (A.1)$$

where x, y and z are the coordinates of the microphone, m, n are the indices of the modes propagating in the tube, a is the width of the tube cross-section, k_{mn} is the modal wavenumber, $k_{mn} = \sqrt{k^2 - \left(\frac{m\pi}{a}\right)^2 - \left(\frac{n\pi}{a}\right)^2}$, $k = \omega/c$ and A_{mn} are the modal excitation coefficient in the incident sound wave and R_{mn} are the unknown modal reflection coefficients which depend on the frequency, on the angle of incidence of the mode and on the acoustical properties of sound-absorbing material. The Fourier transform of Eq.(A.1) is

$$\tilde{p}(K, \omega) = \sum_{m=0}^{\infty} \sum_{n=0}^{\infty} \cos \frac{m\pi}{a} x \cos \frac{n\pi}{a} y \left(A_{mn} \int_{-\infty}^{\infty} e^{i(K-k_{mn})z} dz + A_{mn} R_{mn} \int_{-\infty}^{\infty} e^{i(K+k_{mn})z} dz \right),$$
$$(A.2)$$

where K is the wavenumber.

The analytical simplification of Eq. (A.2) is:

$$\tilde{p}(K, \omega) = \sum_{m=0}^{\infty} \sum_{n=0}^{\infty} \cos \frac{m\pi}{a} x \, \cos \frac{n\pi}{a} y \, \times \cdots$$
$$\cdots \left[A_{mn} \, e^{i(K-k_{mn})\frac{z_2+z_1}{2}} \, (z_2 - z_1) \, \text{sinc} \left((K - k_{mn})\frac{z_2 - z_1}{2} \right) + \cdots \right.$$
$$\left. \cdots A_{mn} \, R_{mn} \, e^{i(K+k_{mn})\frac{z_2+z_1}{2}} \, (z_2 - z_1) \, \text{sinc} \left((K + k_{mn})\frac{z_2 - z_1}{2} \right) \right],$$
$$(A.3)$$

where the infinite limits of the integral are replaced by the first and the last positions, z_1 and z_2, between which the sound pressure measurements were taken. In the above equation $\text{sinc}\, z = \frac{\sin z}{z}$. The unknown coefficients, A_{mn} and R_{mn}, can be recovered by minimising the difference between the measured, $\tilde{p}_m(K, \omega)$,

and predicted, $\tilde{p}(K, \omega, \mathbf{w})$, pressure spectra for every mode and frequency, i.e.:

$$F\left(\omega\right) = \int_K |\tilde{p}_m\left(K, \omega, \right) - \tilde{p}\left(K, \omega, \mathbf{w}\right)|^2 \to 0, \qquad (A.4)$$

where $\mathbf{w} = \{A_{mn}, R_{mn}\}$ is the design vector.

The wavenumber spectra $\tilde{p}_m\left(K_v, \omega\right)$ required for the optimisation process were determined from the experiment which is illustrated in Figure 1. The application of the trapezoidal integration rule to the frequency sound pressure spectra $p_m(z_j, \omega)$ for the $N = 52$ equidistantly spaced microphone positions in the impedance tube yields:

$$\tilde{p}_m(K, \omega) = \int_{-\infty}^{\infty} p_m(z, \omega) e^{iKz} dz \simeq \frac{\Delta}{2} \sum_{j=1}^{N-1} \left[p_m\left(z_{j+1}, \omega\right) e^{iKz_{j+1}} + p_m\left(z_j, \omega\right) e^{iKz_j} \right],$$
$$(A.5)$$

where Δ is the separation between two subsequent microphone positions in the axial direction (i.e. 40 mm), z_j and z_{j+1} are the j-th and j+1-th axial positions, respectively.

The above optimisation process is repeated for each frequency in the acoustic spectra in the given wavenumber range of $K_{min} < K < K_{max}$. This process needs to be applied separately to recover the amplitude and phase data in these two unknown quantities which can be expressed as:

$$A_{mn} = a_{mn} e^{i\phi_{mn}}, \quad A_{mn} R_{mn} = b_{mn} e^{i\psi_{mn}}. \qquad (A.6)$$

This enables us to avoid problems in dealing with complex numbers. Here a_{mn}, b_{mn} are the amplitudes of the forward and backward waves and ϕ_{mn} and ψ_{mn} are their phases, which are real numbers for which the minimisation procedure is easy to converge.

The total absorption coefficient, which does include the energy transmitted by and dissipated through the high order mode absorption mechanisms can be derived from the basic knowledge of the energy relations in a waveguide. Two methods were used to calculate the absorption coefficient were used in this work. The first method makes use of the ratio of incident and reflected energy in the

24

tube, leading to

$$\alpha_{amp}(\omega) = 1 - \frac{\displaystyle\sum_{m'n'} \frac{\mathrm{Re}(k_{m'n'})\|A_{m'n'}R_{m'n'}\|^2}{\varepsilon_{m'}\varepsilon_{n'}}}{\displaystyle\sum_{mn} \frac{\mathrm{Re}(k_{mn})\|A_{mn}\|^2}{\varepsilon_m\varepsilon_n}}, \tag{A.7}$$

For the second method, the total absorption coefficient was calculated using the discrete sound intensity data as:

$$\alpha_{int}(\omega) = 1 - \left| \frac{\int\limits_K I_r(K,\omega)\,dK}{\int\limits_K I_i(K,\omega)\,dK} \right|, \tag{A.8}$$

where K is the wavenumber, and the measured intensities in the incident and the reflected sound waves are:

$$I_i(K,\omega) = \frac{1}{2}\mathrm{Re}\Big(p_i(K,\omega)\,u_i^*(K,\omega)\Big), \ I_r(K,\omega) = \frac{1}{2}\mathrm{Re}\Big(p_r(K,\omega)\,u_r^*(K,\omega)\Big), \tag{A.9}$$

where the asterisk symbol denotes the complex conjugation. The mean sound pressure measured between two closely spaced microphone positions and sound velocity are:

$$p(z_j,\omega) = \frac{1}{2}\Big(p(z_j,\omega) + p(z_{j-1},\omega)\Big), \tag{A.10}$$

$$u(z_j,\omega) = -\frac{1}{i\omega\rho_0\Delta}\Big(p(z_j,\omega) - p(z_{j-1},\omega)\Big), \tag{A.11}$$

where z_j denotes the j-th position of the microphone and Δ is the separation between these two positions.

References

[1] ISO10534-2:1998, Determination of sound absorption coefficient and impedance in impedance tubes, part 2: Transfer-function method, International Organization for Standardization, Geneva, Switzerland.

[2] J.-F. Allard, N. Attala, Propagation of Sound in Porous Media: Modelling Sound Absorbing Materials, Wiley, Chichester, 2009.

[3] K. V. Horoshenkov, A. Khan, Acoustic shielding effect of plants and hedges, (Last accessed on 23/11/2015).
URL http://www.greener-cities.eu/

[4] D. Aylor, Noise reduction by vegetation and ground, leaf width, and breadth of canopy, Journal of Acoustical Society of America 51 (1972) 197–205.

[5] N. H. Wong, A. Y. K. Tan, P. Y. Tan, K. Chiang, N. C. Wong, Acoustics evaluation of vertical greenery systems for building walls, Building Environment 45(2) (2010) 411–420.

[6] K. V. Horoshenkov, Acoustic properties of low growing plants, Journal of Acoustical Society of America 133(5) (2013) 2554–2565.

[7] S. H. Tang, P. P. Ong, H. S. Woon, Monte carlo simulation of sound propagation through leafy foliage using experimentally obtained leaf resonance parameters, Journal of Acoustical Society of America 80(6) (1986) 1740–1744.

[8] ISO354:2003, Measurement of sound absorption in a reverberation room, International Organization for Standardization, Geneva, Switzerland.

[9] J. Prisutova, K. V. Horoshenkov, J.-P. Groby, B. Brouard, A method to determine the acoustic reflection and absorption coefficients of porous media by using modal dispersion in a waveguide, Journal of Acoustical Society of America 136(6) (2014) 2947–2958.

[10] Y. Miki, Acoustic properties of porous materials: Generalization of empirical models, Journal of Acoustical Society of Japan 11 (1990) 25–28.

[11] P. M. Morse, K. U. Ingard, Theoretical acoustics, Princeton University Press, Princeton, 1987.